Progress In Electromagnetics Research M, Vol. 104, 101–110, 2021

Compact Tri-Band Dual-Polarized Shared Aperture Array

Jiachen Xu*, Chenjiang Guo, and Jun Ding

Abstract—In this paper, an S/C/Ku triple-band (TB) dual-polarization (DP) shared aperture array (SAA) with an approximate frequency ratio of $1 : 1.8 : 4.5$ is proposed. An S/C dual-band dual-polarized (DBDP) perforated patch antenna is designed as a shared element, and the S-band array consists of S-band-working shared elements. The C-band array interlaces with C-band-working shared element and C-band cross-patches with phase compensation. The Ku band array consists of dual-polarization rectangular dielectric resonator antennas (DRAs) for its small section area and high design freedom. In order to ensure the symmetry of the structure, all the ports adopt a vertical welding structure. A 1×3 prototype array is fabricated and measured, showing that the S-, C-, and Ku-bands obtain the bandwidths of 2%, 2.1%, and 1.8%, respectively. The polarization isolation is better than 20 dB in all three bands, while the cross-polarization is lower than -20 dB. The proposed array has the advantages of low cost and high integration; moreover, the proposed array owns excellent potential for expansion to large aperture benefited from its symmetry.

1. INTRODUCTION

With the development of radar technology, the requirements for antenna systems are becoming higher and higher [1]. For a Synthetic Aperture Radar (SAR) antenna, a multi-frequency antenna array can provide better reflection or transmission data from different targets, and a dual-polarization antenna array can provide frequency diversity for gathering more information. Besides, people usually want the antenna to have a compact size [2, 3]. Therefore, the dual-/multi-band dual-polarized arrays with shared aperture are attracting more and more attention due to their ability to reduce the size and mass of the SAA with little effect on performance [4, 5].

At present, most SAAs can only achieve dual-bands, and the typical structures are perforated type [4–8], interleaved type [9–11], as well as the latest proposed shared element type [12]. However, there is not much literature on TB SAA due to the difficulty of array arrangement. In [13], TB element is used to form a TB SAA, but the maximum frequency ratio is only 1.8, and it cannot operate in dual-polarizations. Two types of TB SAA are proposed in [14] and [15], respectively, but their antennas of the three bands do not share the aperture sufficiently. Ref. [16] combines the characteristics of perforated type and interleaved types to achieve an actual TB SAA, but there is still room for improvement in scalability.

In this paper, an S/C/Ku TBDP SAA for SAR applications is designed and investigated. We first design an S/C dual-band perforated microstrip antenna as a shared element. Then we combine the characteristics of perforated type, interleaved type, and shared element types SAA to propose the S/C/Ku TBDP SAA. Using the dual-band shared element, the S- and C-band antennas can share the same feed port, which further improves the integration. Moreover, the application of vertical welding makes the structure symmetrical, thus allowing the proposed SAA to have the potential to expand into a large aperture.

Received 23 July 2021, Accepted 20 August 2021, Scheduled 25 August 2021

* Corresponding author: Jiachen Xu (xujiachen9151@outlook.com).

The authors are with the School of Electronics and Information, Northwestern Polytechnical University, Xi'an 710129, People's Republic of China.

2. DESIGN OF THE TBDP SAA

2.1. Configuration

This paper combines the perforated type, interleaved type, and shared element type SAA to propose a novel S/C/Ku TBDP SAA operating at 3 GHz/5.3 GHz/13.6 GHz, respectively. Fig. 1 shows the overall structure of the proposed TBDP SAA (only 1×3 prototype arrays are discussed in this paper, as Fig. 2 shows). Due to structural constraints, the array element spacing of Ku-/C-/S-band has a relationship of $1 : 2 : 4$. In order to avoid mutual coupling and appearing grating lobe, meanwhile, we also want the array to have a compact size, so the element spacing $lku = lc/2 = ls/2 = 15\,\text{mm} = 0.6\lambda s = 0.53\lambda c = 0.68\lambda ku$ is selected. In the 1×3 prototype SAA, we design an S/C dual-band perforated patch antenna as a shared element, and the S-band consists of two S-band-working shared elements. Meanwhile, the C-band array consists of two C-band-working shared elements and a C-band cross-patch with phase compensation to ensure a suitable element spacing. At Ku-band, we use a slot coupled DP DRA as the Ku-band element because it is a high design freedom antenna with a small base area; moreover, it does not require an additional substrate and does not affect the design of other bands. Each four DRAs act as a sub-array and are fed by a pair of power dividers.

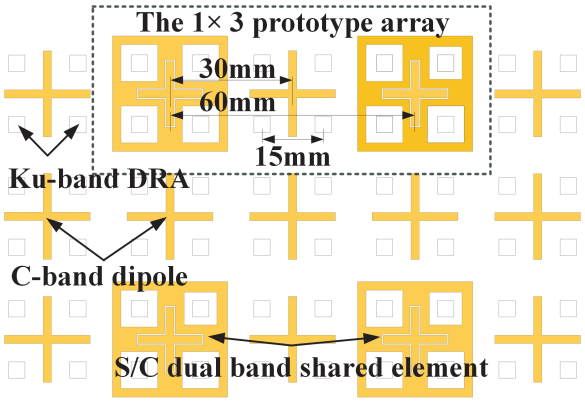

Figure 1. Array arrangement of the proposed TBDP SAA.

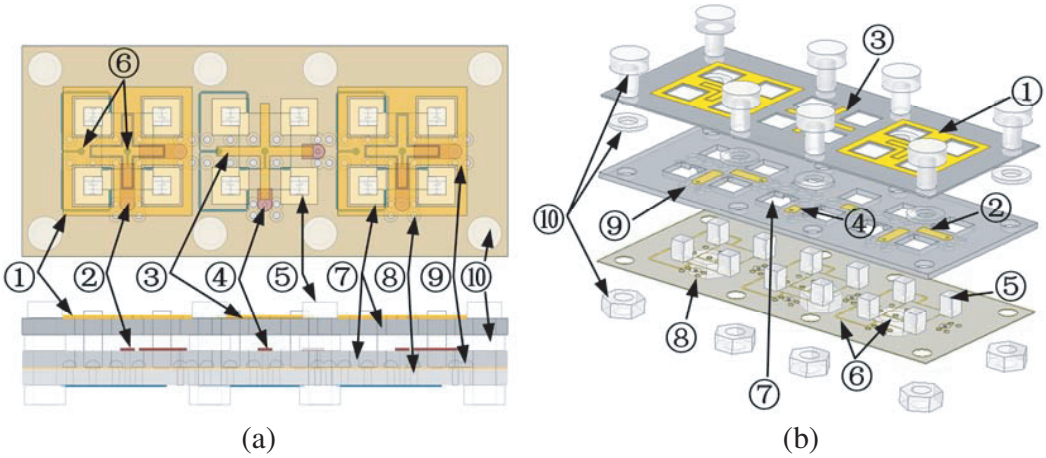

Figure 2. Configuration of the proposed TBDP SAA. ① S/C dual band shared element, ② S/C-band feedline, ③ C-band dipole, ④ C-band feedline, ⑤ Ku-band DRAs, ⑥ Ku-band fed networks, ⑦ notches on Sub2 & Sub3, ⑧ holes for SMA, ⑨ blind holes, ⑩ threaded parts. (a) Top and side view. (b) 3D view.

The SAA contains three layers of substrates; the Sub1 is a 0.25 mm thick F4BM265 substrate ($\varepsilon_r = 2.65$) and placed at the bottom; the lower side prints Ku-band power dividers while the upper side prints the GND and feeding slot. Sub2 is a 1.5 mm thick F4BM350 substrate ($\varepsilon_r = 3.5$) placed on top of sub1, and the upper side prints the feed lines for the shared element and C-band cross-patch. Moreover, we select vertical soldering to ensure that the edges of the array are flat, and the SAA can be easily expanded, so we need to process some blind holes in the lower side of Sub2 for accommodating the solders. The sub3 employs a 0.5 mm thick F4BM220 ($\varepsilon_r = 2.2$) substrate with S/C shared elements and C-band cross-patch printed on the upper side; in addition, we set a 1 mm air layer between Sub2 and Sub3 for impedance matching. The Ku-band DRAs (Al_2O_3, $\varepsilon_r = 9.6$) are glued in the upper side of sub1, so we need to make some square perforations in Sub2 and Sub3, respectively.

2.2. S/C Dual-band Shared Element

Figure 3 shows the configuration of the S/C DBDP perforated patch antenna (shared element). The shared element employs a centrosymmetric structure to achieve dual-polarization conveniently and is fed by two orthogonal proximity coupled microstrip lines. The following equation can approximately calculate the length of the S/C dual-band patch,

$$Sl1 \approx \frac{c}{2f_0\sqrt{\varepsilon_{eff}}} \tag{1}$$

where $Sl1$ is the length of the shared element shown in Fig. 3, c the light speed in free space, ε_{eff} the effective dielectric constant, and f_0 the centre frequency at 3 GHz in this design.

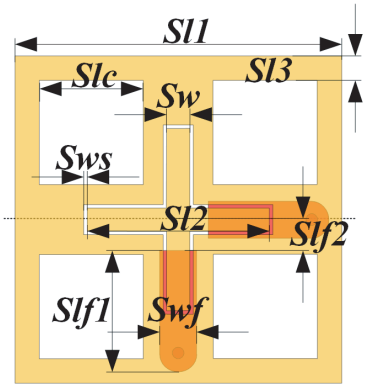

Figure 3. Configuration of the shared element, $Sl1 = 28.2$ mm, $Sl2 = 15.72$ mm, $Sl3 = 2.1$ mm, $Sw = 2$ mm, $Sws = 0.3$ mm, $Slc = 9$ mm, $Slf1 = 10.5$ mm, $Slf2 = 2.6$ mm, $Swf = 3.2$ mm.

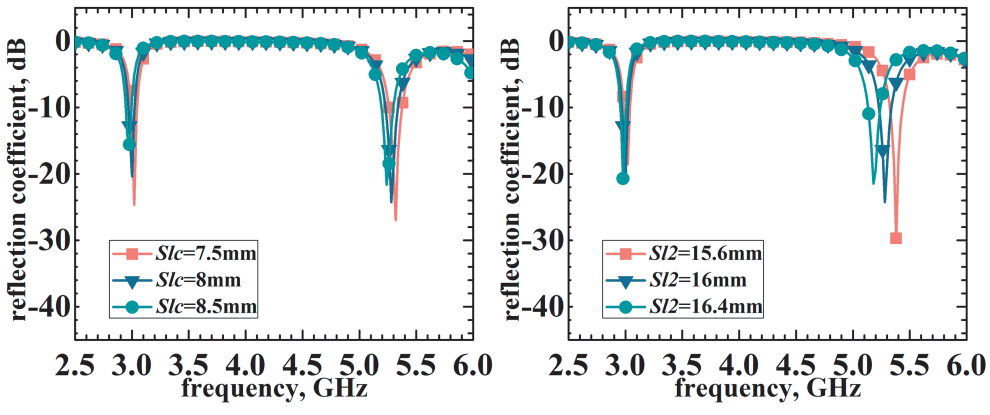

Figure 4. (a) Simulated reflection coefficient of the shared element with different values of Slc. (b) Simulated reflection coefficient of the shared element with different values of $Sl2$.

We etch four square perforations in the antenna to set the Ku DRAs, and the perforation size will affect the resonant frequency of the antenna. Fig. 4(a) shows the simulated reflection coefficient of the S/C shared element with different values of the perforation size (Slc). We can observe that the two resonant frequencies of the antenna decrease slightly with the increase of the perforation size. A larger perforation size can reduce the impact of shared elements on Ku DRAs, but it will reduce the antenna bandwidth, and the value of 8 mm is chosen here. In order to generate another resonant frequency, we etch a crossed annular slot at the centre of the perforated patch and analyze the critical parameter $Sl2$ of the annular slot. Fig. 4(b) shows the simulated reflection coefficient of the S/C shared element with different values of $Sl2$. We can see that when $Sl2$ increases, the low-frequency resonance point is almost constant, while the high-frequency resonance point decreases. An optimized value of 15.72 mm is chosen here.

Figure 5 shows the simulated vector current distribution of the S/C shared element at S- and C-bands. At 3 GHz, strong current distribution is on both sides of the patch, proving that the antenna works in the fundamental mode. At 5.3 GHz, most of the current is distributed at the centre around the cross annular slot, proving that the crossed annular slot produces the second resonant frequency.

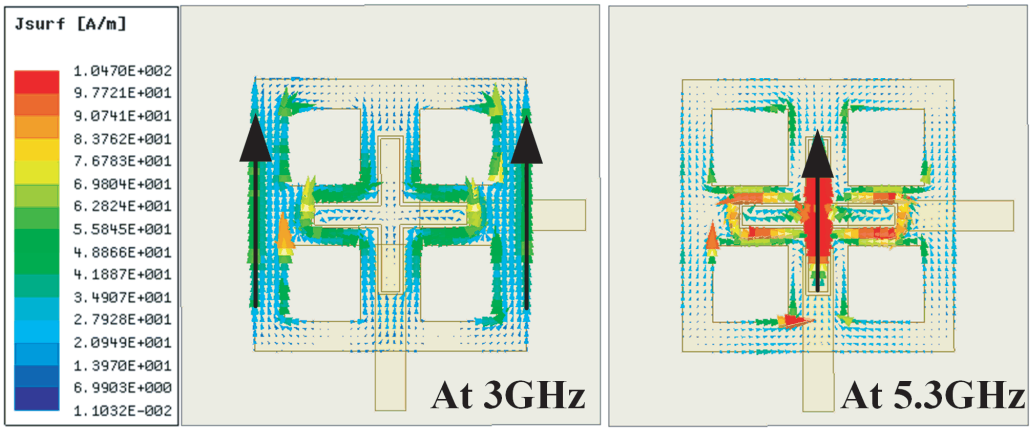

Figure 5. Simulated vector current distribution of the S/C shared element at 3 GHz and 5.3 GHz.

2.3. C-Band Element

The C-band element employs the proximity coupled cross-patch for the following reasons: compact size, ease of being interlaced with Ku-band DRAs, and same feed scheme as dual-band shared element. The length of cross-patch ($Cl1$) can refer to Equation (1) for calculating $Sl1$ [16]. Fig. 6 shows the details of the C-band element. Since the C-band array contains two types of elements, it is necessary to analyze

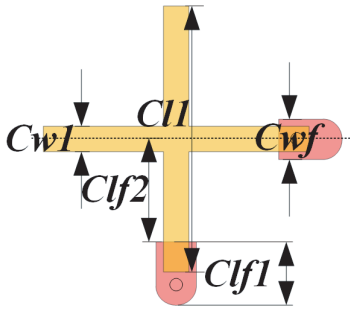

Figure 6. Configuration of the C-band cross-patch, $Cl1 = 20.88$ mm, $Cw1 = 2$ mm, $Clf1 = 5$ mm, $Clf2 = 8.1$ mm, $Cwf = 3.2$ mm.

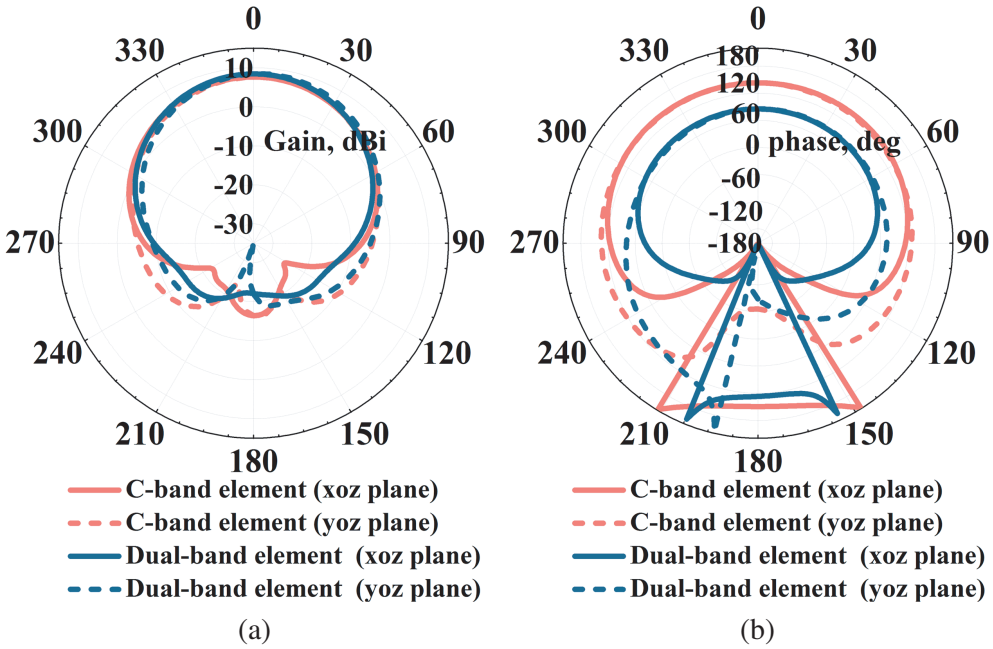

Figure 7. Comparison chart of radiation characteristics. (a) Radiation pattern. (b) Phase pattern.

their radiation performance separately, and Fig. 7 shows the comparison chart. We can see that the two types of elements have similar radiation patterns, but the C-band cross-patch has a 50° phase advance over the shared-element, so a 50° phase delay of the C-band cross-patch is required when this hybrid array is fed.

2.4. Ku-Band Array

Figure 8 shows the detail of Ku-band DRA and feed networks. We use "H" and "I" shaped slots to reduce the slot length and improve the polarization isolation [17], and the design detail can refer to [18]. Furthermore, each four DRAs are arranged in the way of "pair-wise" anti-phase feed to reduce cross-

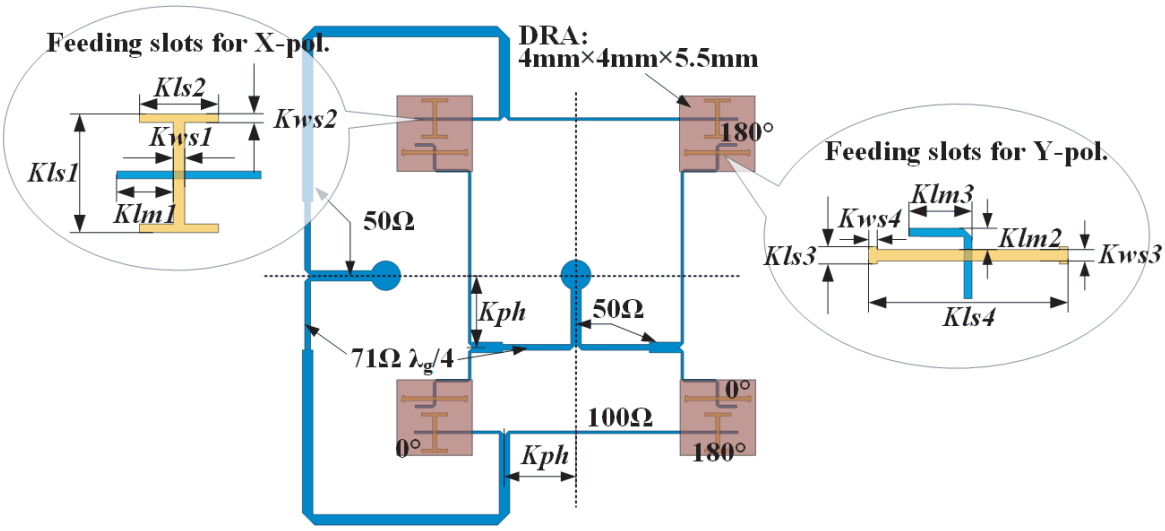

Figure 8. Configuration of the Ku-band DRA and feed networks, $Kls1 = 2.07$ mm, $Kls2 = 1.38$ mm, $Kls3 = 3.48$ mm, $Kls4 = 0.3$ mm, $Kws1 = 0.2$ mm, $Kws2 = 0.15$ mm, $Kws3 = 0.2$ mm, $Kws4 = 0.15$ mm, $Klm1 = 0.98$ mm, $Klm2 = 0.4$ mm, $Klm3 = 1.1$ mm, $Kph = 3.8$.

polarization. Since the Ku-band DRA is very small, the space left for the feed network is very crowded. Moreover, the power dividers have to avoid the welding position of the S-/C-band SMA connectors, so we use the 100 Ω feed lines to match the antennas for relieving the congestion of the feed networks.

2.5. Mutual Coupling Analysis

Since the arrays of three bands radiate through the same aperture, it is necessary to analyze the volume current density distribution of the proposed TBDP SAA at each band, as shown in Fig. 9. At 3 GHz, the current mainly distributes at the edge of the shared elements, while the current distribution on C-band cross-patch and Ku-band DRAs is weak. At 5.3 GHz, the strong E field is distributed at the centre of the shared element as well as C-band cross-patch and almost no current distribution on Ku-band DRA. At 13.6 GHz, there is a strong current distribution at the twelve Ku DRAs, but the minimal current is distributed at shared elements and C-band cross-patch. The current distribution analysis reveals low mutual coupling between different bands, and the antenna can work individually at each band.

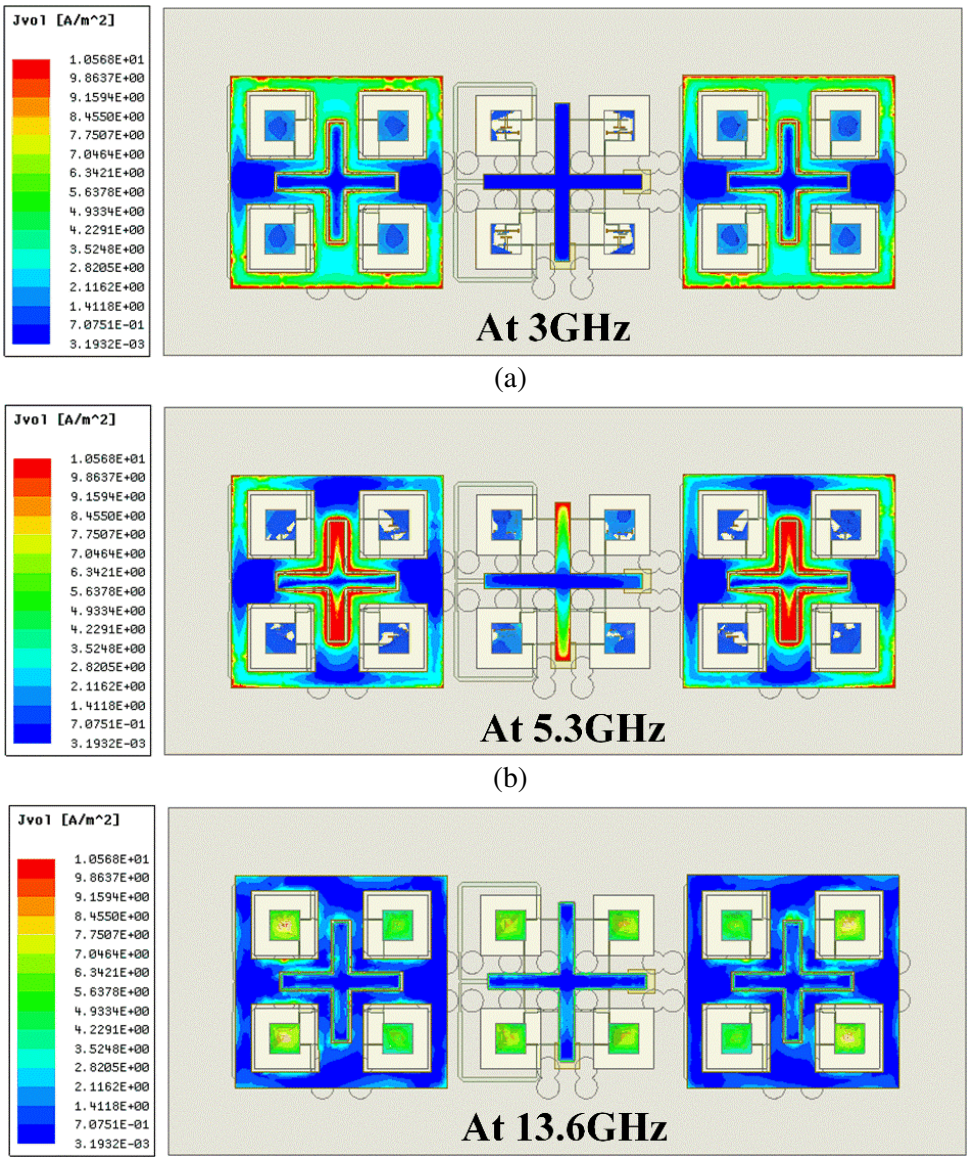

Figure 9. Volume current density distribution of the TBDP SAA. (a) At 3 GHz. (b) At 5.3 GHz. (c) At 13.6 GHz.

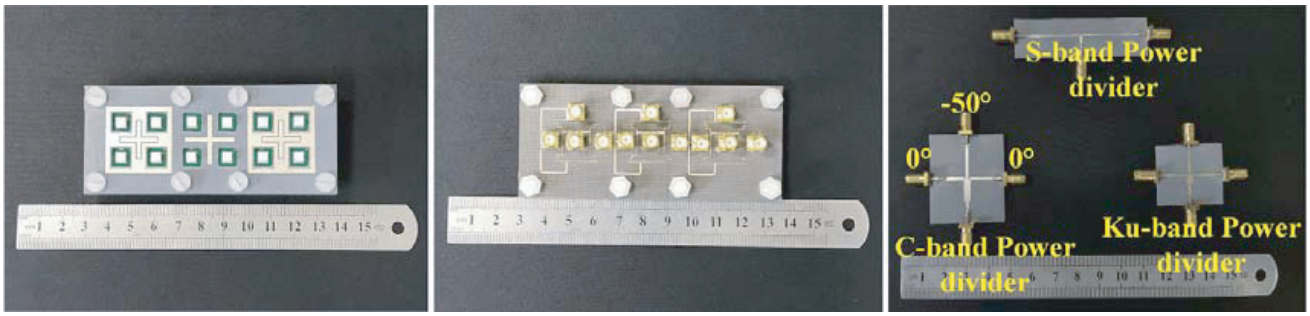

(a) (b) (c)

Figure 10. The fabricated antenna and the matching power dividers. (a) Top view of the TBDP SAA. (b) Bottom view of the SAA. (c) Three power dividers for the prototype array.

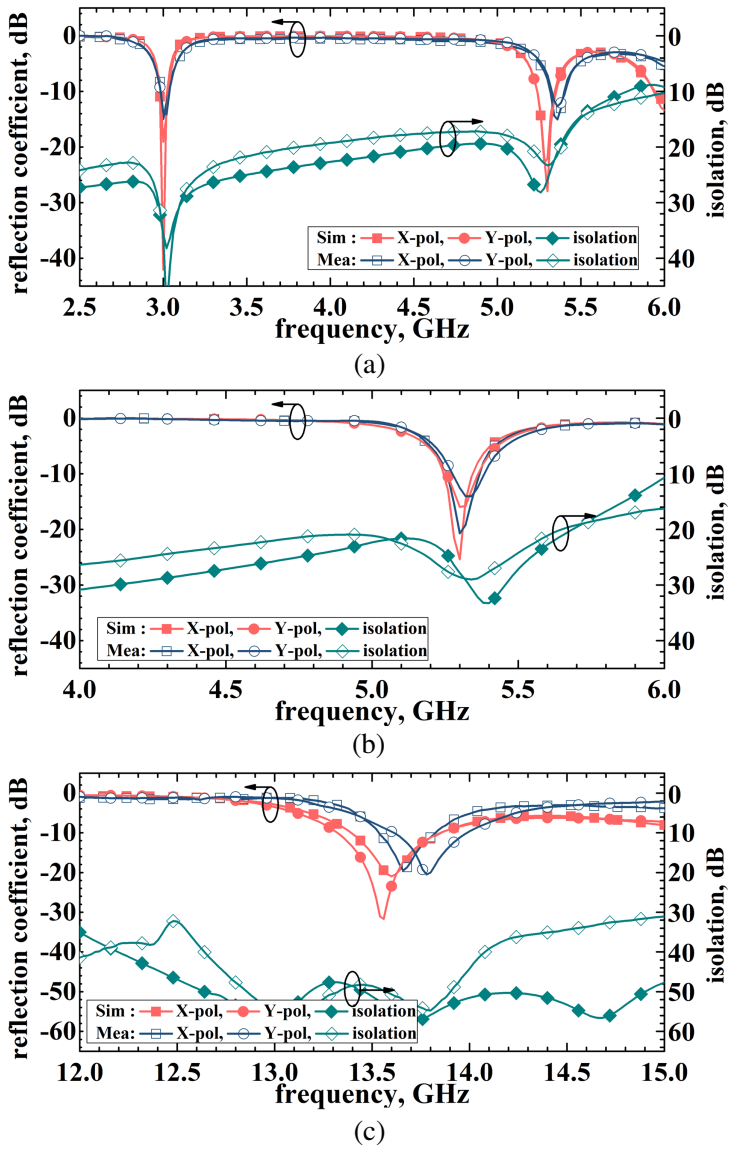

Figure 11. Measured and simulated S-parameter. (a) S-band. (b) C-band. (c) Ku-band.

3. RESULTS AND DISCUSSION

To validate the design, we fabricated and measured the proposed array. Fig. 10 shows the prototype array and the matching power dividers, while Figs. 11–12 show the simulated and measured data.

Figure 11 shows the simulated/measured reflection coefficient of the prototype array. In Fig. 11(a), we can see that the shared element covers the bands of 2.97–3.03 GHz and 5.31–5.42 GHz. The lower frequency is in good agreement with the simulation data. However, in the higher band, there is a 70 MHz frequency shift on the resonance points between simulated and measured results, and it may be that the thickness of the air layer between sub2 and sub3 is not accurate enough. The isolation between polarizations is better than 22 dB. Fig. 10(b) shows that the C-band cross-patch achieves a measured bandwidth from 5.26 to 5.38 GHz, and the polarization isolation is better than 24 dB, which agrees reasonably well with the simulations. For the Ku-band, the measured reflection coefficient below -10 dB from 13.6 to 13.84 GHz is achieved, and the isolation between two ports is better than 40 dB. Compared with the measured data, the simulated data of X-port lose about 210 MHz bandwidth, and Y-port has about 300 MHz frequency shift up. The existence of deviation is mainly caused by machining and welding errors. Moreover, the antenna in Ku-band is more sensitive to errors.

The simulated and measured radiation patterns are shown in Fig. 12. In all three bands, the simulated and measured co-polarization patterns show good agreement. The measured cross-polarization is better than -22 dB, -20 dB, and -25 dB at S-/C-/Ku-band, respectively, which is worse than the simulated data. Because the cross-polarization is more sensitive to machining deviation and limited measurement accuracy.

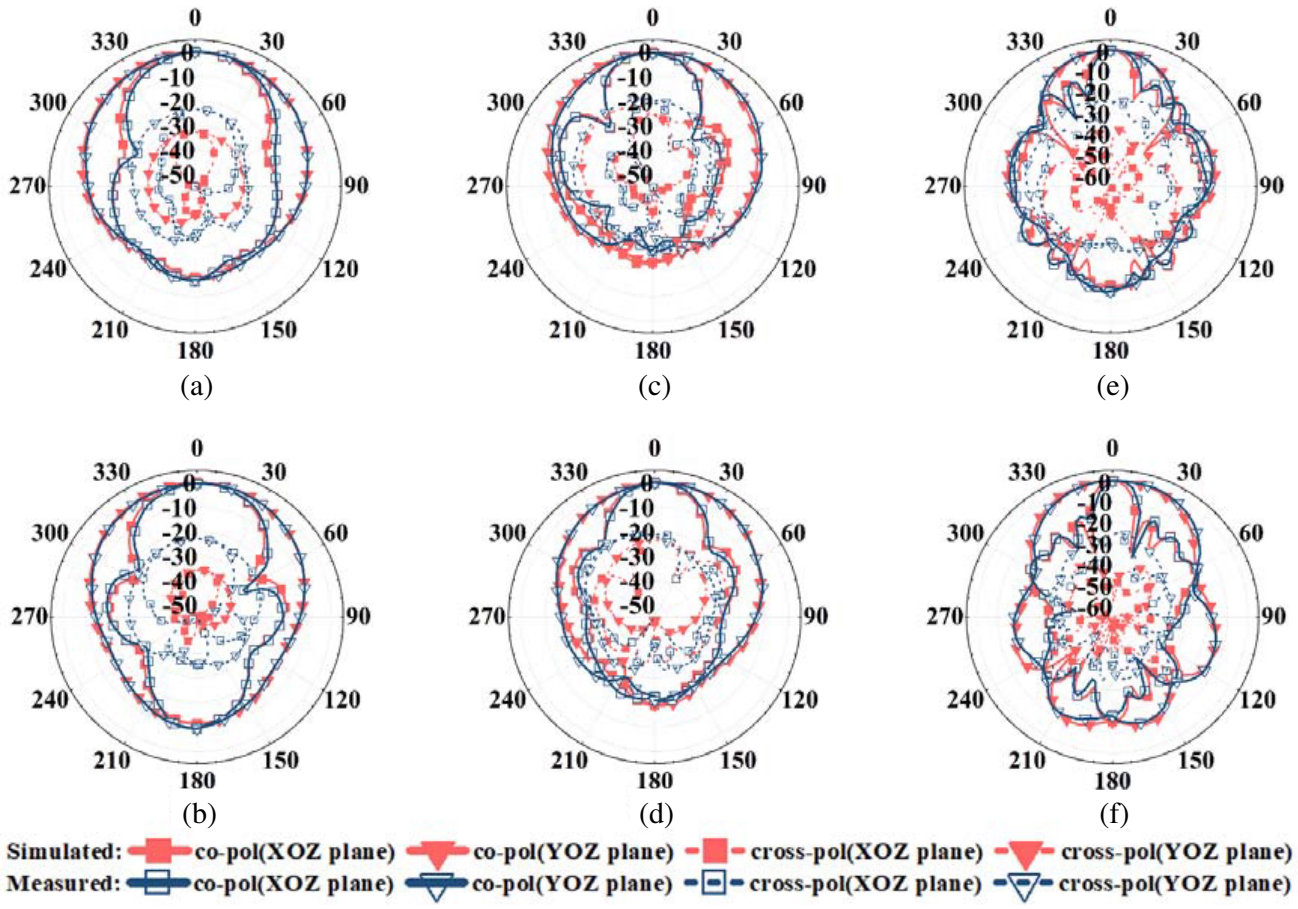

Figure 12. Measured and Simulated radiation patterns, (a) S-band, X-polarization; (b) S-band, Y-polarization; (c) C-band, X-polarization; (d) C-band, Y-polarization; (e) Ku-band, X-polarization; (f) Ku-band, Y-polarization.

4. CONCLUSION

This paper combines perforated type, interleaved type, and shared element types SAA to propose a novel S/C/Ku TBDP SAA. An S/C dual-band perforated microstrip antenna is designed as a shared element. Furthermore, the S-band array consists of two S-band-working shared elements; the C-band array is interleaved by two C-band-working shared elements and a C-band cross-patch with phase compensation; the Ku band array consists of DP DRAs. The S- and C-band antennas can share the same feed port by using the dual-band shared element, which further improves the integration. Moreover, the application of vertical welding makes the structure symmetrical, thus allowing the proposed SAA to have the potential to expand into a large aperture. The proposed antenna array is fabricated and measured, covering the frequency bands of 2.97–3.03 GHz, 5.31–5.42 GHz, and 13.6–13.84 GHz with the reflection coefficient below −10 dB; the isolations between bands are over 22 dB; the cross-polarization level for both bands is lower than −20 dB in the main lobe. The proposed antenna has the advantages of low cost, high integration, and the potential to expand into a large array, making it very suitable for the modern SAR antenna system.

REFERENCES

1. Rocca, P., M. Donelli, G. Oliveri, F. Viani, and A. Massa, "Reconfigurable sum-difference pattern by means of parasitic elements for forward-looking monopulse radar," *IET Radar, Sonar and Navigation*, Vol. 7, No. 7, 747–754, 2013.
2. Donelli, M. and P. Febvre, "An inexpensive reconfigurable planar array for Wi-Fi applications," *Progress In Electromagnetics Research C*, Vol. 28, 71–81, 2012.
3. Donelli, M., T. Moriyama, and M. Manekiya, "A compact switched-beam planar antenna array for wireless sensors operating at Wi-Fi band," *Progress In Electromagnetics Research C*, Vol. 83, 137–145, 2018.
4. Shafai, L. L., W. A. Chamma, M. Barakat, P. C. Strickland, and G. Seguin, "Dual-band dual-polarized perforated microstrip antennas for SAR applications," *IEEE Transactions on Antennas and Propagation*, Vol. 48, No. 1, 58–66, 2000.
5. Pozar, D. M. and S. D. Targonski, "A shared-aperture dual-band dual-polarized microstrip array," *IEEE Transactions on Antennas and Propagation*, Vol. 49, No. 2, 150–157, 2001.
6. Sun, Z., K. P. Esselle, S.-S. Zhong, and Y. J. Guo, "Shared-aperture dual-band dual-polarization array using sandwiched stacked patch," *Progress In Electromagnetics Research C*, Vol. 52, 183–195, 2014.
7. Vetharatnam, G. and V. C. Koo, "Compact L- & C-band SAR antenna," *Progress In Electromagnetics Research Letters*, Vol. 8, 105–114, 2009.
8. Kim, J. H., S. K. Hong, and B. G. Kim, "A shared-aperture S/X dual broadband microstrip antenna with one perforated patch," *Microwave and Optical Technology Letters*, Vol. 62, No. 1, 507–513, 2020.
9. Xu, J. C., B. Z. Lan, J. K. Zhang, C. J. Guo, and J. Ding, "A novel dual-band dual-polarized shared-aperture antenna with high isolation," *International Journal of Microwave and Wireless Technologies*, Vol. 12, No. 7, 652–659, 2020.
10. Qu, X., S. S. Zhong, Y. M. Zhang, and W. Wang, "Design of an S/X dual-band dual-polarised microstrip antenna array for SAR applications," *IET Microwaves Antennas & Propagation*, Vol. 1, No. 2, 513–517, 2007.
11. Mao, C. X., S. Gao, Y. Wang, Q. X. Chu, and X. X. Yang, "Dual-band circularly polarized shared-aperture array for C-/X-band satellite communications," *IEEE Transactions on Antennas and Propagation*, Vol. 65, No. 10, 5171–5178, 2017.
12. Xu, J. C., C. J. Guo, and J. Ding, "Dual-band orthogonal polarised shared aperture array with shared-elements," *Electronics Letters*, Vol. 57, No. 5, 197–199, 2021.

13. Li, M., Y. Wu, M. Qu, L. X. Jiao, and Y. N. Liu, "Triband planar shared-aperture antenna array with similar-shaped radiation patterns," *Microwave and Optical Technology Letters*, Vol. 60, No. 9, 2284–2288, 2018.
14. Zhong, S. S., Z. Sun, L. B. Kong, C. Gao, W. Wang, and M. P. Jin, "Tri-band dual-polarization shared-aperture microstrip array for SAR applications," *IEEE Transactions on Antennas and Propagation*, Vol. 48, No. 1, 4157–4165, 2012.
15. Li, K., T. Dong, and Z. Xia, "A broadband shared-aperture L/S/X-band dual-polarized antenna for SAR applications," *IEEE Access*, Vol. 7, 51417–51425, 2019.
16. Mao, C. X., S. Gao, Q. Luo, T. Rommel, and Q. X. Chu, "Low-cost X/Ku/Ka-band dual-polarized array with shared aperture," *IEEE Transactions on Antennas and Propagation*, Vol. 65, No. 7, 3520–3527, 2017.
17. Gao, S. and A. Sambell, "Low-cost dual-polarized printed array with broad bandwidth," *IEEE Transactions on Antennas and Propagation*, Vol. 52, No. 12, 3394–3397, 2004.
18. Guo, Y. X. and K.-M. Luk, "Dual-polarized dielectric resonator antennas," *IEEE Transactions on Antennas and Propagation*, Vol. 51, No. 5, 1120–1123, 2003.